

# The Proper Motion of the Large Magellanic Cloud: A Reanalysis

Mario H. Pedreros<sup>1</sup>

*Departamento de Física, Facultad de Ciencias, Universidad de Tarapacá, Casilla 7-D, Arica, Chile*

`mpedrero@uta.cl`,

and

Edgardo Costa<sup>1</sup> and René A. Méndez<sup>1</sup>

*Departamento de Astronomía, Universidad de Chile, Casilla 36-D, Santiago, Chile*

`[costa, rmendez]@das.uchile.cl`

## ABSTRACT

We have determined the proper motion (PM) of the Large Magellanic Cloud (LMC) relative to four background quasi-stellar objects, combining data from two previous studies made by our group, and new observations carried out in four epochs not included the original investigations. The new observations provided a significant increase in the time base and in the number of frames, relative to what was available in our previous studies. We have derived a total LMC PM of  $\mu = (+2.0 \pm 0.1)$  mas yr<sup>-1</sup>, with a position angle of  $\theta = (62.4 \pm 3.1)^\circ$ . Our new values agree well with most results obtained by other authors, and we believe we have clarified the large discrepancy between previous results from our group. Using published values of the radial velocity for the center of the LMC, in combination with the transverse velocity vector derived from our measured PM, we have calculated the absolute space velocity of the LMC. This value, along with some assumptions regarding the mass distribution of the Galaxy, has in turn been used to calculate the mass of the Milky Way. Our measured PM also indicates that the LMC is not a member of a proposed stream of galaxies with similar orbits around our galaxy.

*Subject headings:* astrometry: proper motions — quasars — Large Magellanic Cloud

---

<sup>1</sup>Visiting Astronomer, Cerro Tololo Inter-American Observatory, National Optical Astronomy Observatories, operated by the Association of Universities for Research in Astronomy, Inc. (AURA), under cooperative agreement with the National Science Foundation.

## 1. INTRODUCTION

The present study is a follow-up of the works by Anguita, Loyola & Pedreros (2000, hereafter ALP) and Pedreros, Anguita & Maza (2002, hereafter PAM) in which the PM of the LMC was determined using the "quasar method". This method, fully described in ALP and PAM, consists in using quasi-stellar objects (QSOs) in the background field of the LMC, as fiducial reference points to determine its PM. In this method, the position of the background QSOs is measured at different epochs with respect to bona-fide field stars of the LMC which define a local reference system (hereafter LRS). Because a QSO can be considered a fiducial reference point, any motion detected will be a reflexion of the motion of the LRS of LMC stars.

As shown in Table 1, there is a rather large discrepancy, particularly in Decl., between the PM of the LMC derived by ALP and that derived by PAM, with ALP–PAM differences of  $-0.3 \text{ mas yr}^{-1}$  ( $1.5 \sigma$ ) in R.A., and  $2.5 \text{ mas yr}^{-1}$  ( $12.5 \sigma$ ) in Decl. This difference prompted us to add new epochs to our database (using the same equipment and set-up used by ALP and PAM) and to make a full reanalysis of the entire data set.

Here we report the results obtained combining data from previous studies by our group, with new observations carried out in three additional epochs (not included in the original investigation), for the LMC quasar fields Q0459-6427, Q0557-6713, Q0558-6707, and Q0615-6615 (in the same nomenclature used by ALP and PAM). The original study of field Q0459-6427 was reported in PAM, and those of Q0557-6713, Q0558-6707 and Q0615-6615 in ALP. As can be seen in Table 2, which summarizes the total observational material used in the present paper, our new data provides a significant increase, in time base and in the number of frames, relative to what was available in ALP and PAM. The increase in time base for the fields Q0459-6427, Q0557-6713, Q0558-6707 and Q0615-6615 was 19%, 65%, 126% and 65%, respectively. The corresponding increase in data points was 7%, 18%, 59% and 56%, respectively.

## 2. OBSERVATIONS AND REDUCTIONS

The new observations were carried out with a  $24\mu$  pixels Tektronix 1024x1024 CCD detector attached to the Cassegrain focus of the CTIO 1.5 m telescope in its f/13.5 configuration (scale:  $0.24''/\text{pixel}$ ). Only astrometric observations were secured. Because for each QSO field we adopted the same LRS used by ALP or PAM, there was no need for additional photometric observations. Finding charts for the reference stars and the background QSO in each field can be found in ALP or PAM. As was done in our previous studies, the astrometric observations were made using a Kron-Cousins *R*-band filter, in order to minimize differential color refraction effects.

The method used for the determination of the LMC's PM is the same as that explained in ALP and PAM. Only data not included in those two previous studies went through the full reduction procedure. For data already included in those studies, we used the available raw coordinates for the

centroids of the reference stars and background QSOs. Both, the existing and the newly determined raw coordinates, were treated by means of the same custom programs used in PAM.

In brief, the (x,y) coordinates of the QSO and the LMC field reference stars in each image were determined using the DAOPHOT package (Stetson 1987), and then corrected for differential color refraction and transformed to barycentric coordinates. Then, by averaging the barycentric coordinates of the best set of consecutive images taken of each QSO field throughout our program, a standard reference frame (SRF) was defined for every field. All images, taken at different epochs, of each field, were then referred to its corresponding SRF. This was done through multiple regression analysis by fitting both sets of coordinates to quadratic equations of the form:  $X = a_0 + a_1x + a_2y + a_3x^2$ ;  $Y = b_0 + b_1x + b_2y + b_3x^2$ ; where (X,Y) are the coordinates on the SRF system and (x,y) are the the observed barycentric coordinates. It was found that the above transformation equations yielded the best results for the registration into the SRF, showing no remaining systematic trends in the data.

### 3. RESULTS

Tables 3-6 list the residual PM (relative to the barycenter of the field’s SRF) and photometry (this latter from ALP or PAM, and included here for completeness) of the stars defining the LRS in each of our four QSO fields. Star IDs are the same as those in PAM and ALP, for the corresponding fields. The PM uncertainties correspond to the error in the determination of the slope of the best-fit line. Inspection of these tables shows that the PM uncertainty of most of the reference stars is comparable to, or larger than, their derived PM value, implying that these PM do not represent internal motions in the LMC.

In Figure 1 we present the PM maps for the reference stars listed in Tables 3-6. The dispersion around the mean turned out to be  $\pm 0.34$ ,  $\pm 0.79$ ,  $\pm 0.54$ , and  $\pm 0.41$  mas yr<sup>-1</sup> in R.A., and  $\pm 0.52$ ,  $\pm 0.71$ ,  $\pm 0.58$ ,  $\pm 0.62$  mas yr<sup>-1</sup> in Decl., for Q0459-6427, Q0557-6713, Q0558-6707 and Q0615-6615, respectively. Based on the above argument, the scatter seen in the plots probably stems entirely from the random errors in the measurements, and does not represent the actual velocity dispersion in the LMC.

In Figure 2 we present position *vs.* epoch diagrams for the QSO fields in R.A. ( $\Delta\alpha\cos\delta$ ) and Decl. ( $\Delta\delta$ ), where  $\Delta\alpha\cos\delta$  and  $\Delta\delta$  represent the positions of the QSOs on different CCD frames, relative to the barycenter of the SRF. These diagrams were constructed using individual position data for the QSO in each CCD image as a function of epoch. In Table 7 we give, for each epoch, the mean barycentric positions of the QSOs along with their mean errors, the number of points used to calculate the mean for each coordinate, and the CCD detectors used. Symbol sizes in Figure 2 are proportional to the number of times the measurements yielded the same coordinate value for a particular epoch. The best-fit straight lines resulting from simple linear regression analysis on the data points are also shown. The negative values of the line slopes correspond to the measured PM

of the barycenter of the LRS, in each QSO field, relative to the SRF.

Table 8 summarizes our results for the measured PM of the LMC. Column (1) gives the quasar identification, columns (2) and (3) the R.A. and Decl. components of the LMC’s PM (together with their standard deviations) respectively, and, finally, columns (4), (5) and (6) the number of frames, the number of epochs, and the observation period, respectively. It should be noted that the rather small quoted errors for the PM come out directly from what the least-square fit yields as the uncertainty in the determination of the slope of the best fit line.

#### 4. COMPARISON TO OTHER PROPER MOTION WORK

Table 9 lists the results of all available measurements of the LMC’s PM having uncertainties smaller than  $1 \text{ mas yr}^{-1}$  in both components, as well as the reference system used in each case. With the exception of those cases noted as “Field” in the first column, all the PM listed in Table 9 are relative to the LMC’s center. To facilitate comparisons, we present our current results in both ways. As explained in the next section, our PM values relative to the LMC’s center were obtained correcting the field PM for the rotation of the plane of the LMC.

Our results are in reasonable agreement with most of the available data. They agree particularly well with those of Kroupa et al. (1994), who used the Positions and Proper Motions Star Catalog (PPM, Röser et al., 1993) as reference system, and also with the HST unpublished result of Kallivayalil et al. (2005), who used QSOs as reference system. On the other hand, there still is a significant discrepancy with ALP’s result in Decl. We will further discuss this issue in §6.

In Table 9 we have not included a recent determination of the LMC’s PM by Momany & Zaggia (2005) using the USNO CCD Astrograph all-sky Catalog (UCAC2, Zacharias et al. 2004), because, as confirmed by the errors declared by the authors themselves ( $\sim 3 \text{ mas}$  in both coordinates), the internal accuracy of their methodology is not comparable with ours. Numerous tests carried out by our group, favor the use of fiducial reference points in combination with a LRS defined by relatively few, well studied (bona-fide members, free of contamination from neighboring stars, good signal-to-noise, etc.) LMC stars, to determine a PM of this nature. Interestingly, their result  $[\mu_\alpha \cos \delta, \mu_\delta] \sim [+0.84, +4.32] \text{ mas yr}^{-1}$  is in reasonable agreement with that of ALP.

Combining the components given in the last entry of Table 9, we derive a total LMC PM of  $\mu = (+2.0 \pm 0.1) \text{ mas yr}^{-1}$ , with a position angle of  $\theta = (62.4 \pm 3.1)^\circ$ , measured eastward from the meridian joining the center of the LMC to the north celestial pole. This result is compatible (particularly the PM’s absolute value) with theoretical models (Gardiner et al. 1994), which predict a PM for the LMC in the range  $1.5\text{--}2.0 \text{ mas yr}^{-1}$ , with a position angle of  $\theta \approx 90^\circ$ .

## 5. SPATIAL VELOCITY OF THE LMC AND MASS OF THE GALAXY

Using the PM of the LMC determined in §3, and the radial velocity of the center of the LMC (adopted from the literature), we can calculate the radial and transverse components of the velocity for the LMC, as seen from the center of the Galaxy, along with other parameters described below. To do this we basically followed the procedure outlined by Jones et al. (1994). In the calculations we used as basic LMC parameters those given in Table 8 of ALP, and assumed a rotational velocity  $v_\Phi = 50 \text{ km s}^{-1}$  and a radial velocity  $V_r = 250 \text{ km s}^{-1}$  for the LMC.

In order to determine, from our measured PM values, the space velocity components of the LMC, and its PM with respect to the Galactic Rest Frame (GRF), a series of steps were required. These include: 1. A correction to our measured PM values to account for the rotation of the plane of the LMC; 2. A transformation of the corrected PM into transverse velocity components with respect to the center of the LMC, the Sun, the LSR and the center of the Galaxy; both in the equatorial and galactic coordinate systems. These transverse velocities, in combination with the radial velocity of the center of the LMC (adopted from the literature), allowed us to derive the components of the space velocity of the LMC corrected for the Sun’s peculiar motion relative to the LSR, and also corrected for the velocity of the LSR itself, relative to the center of the Galaxy. The above calculations were made using an *ad-hoc* computer program, developed by one of the authors (MHP), which generates results consistent with those from an independent software (Piatek, 2005; private communication).

The results of the above procedure applied to our four quasar fields are presented in Table 10. In rows 1-2 we list the R.A. and Decl. corrections to our measured PM to account for the rotation of the plane of the LMC, and in rows 3-4, the corresponding corrected PM values, in equatorial coordinates, as viewed by an observer located at the center of the LMC. In rows 5-8 we give calculated PM values relative to the GRF, both in equatorial and galactic coordinates. These values correspond to the LMC’s PM as seen by an observer located at the Sun, with the contributions to the PM, from the peculiar solar motion and from the LSR’s motion, removed. In rows 9-11 we give the  $\Pi$ ,  $\Theta$  and  $Z$  components of the space velocity in a rectangular cartesian coordinate system centered on the LMC (as defined by Schweitzer et al., 1995, for the Sculptor dSph). The  $\Pi$  component is parallel to the projection onto the Galactic plane of the radius vector from the center of the Galaxy to the center of the LMC, and is positive when it points radially away from the Galactic center. The  $\Theta$  component is perpendicular to the  $\Pi$  component, parallel to the Galactic plane, and points in the direction of rotation of the Galactic disk. The  $Z$  component points in the direction of the Galactic north pole. These three components are free from the Sun’s peculiar motion and LSR motion. In rows 12-13 we give the LMC’s radial and transverse space velocities, as seen by an hypothetical observer located at the center of the Galaxy, and at rest with respect to the Galactic center.

All of the above calculations were carried out assuming a distance of 50.1 kpc of the LMC from the Sun, a distance of 8.5 kpc of the Sun from the Galactic center, a  $220 \text{ km s}^{-1}$  circular velocity of the LSR and a peculiar velocity of the Sun relative to the LSR of  $(u_{\odot}, v_{\odot}, w_{\odot}) = (-10, 5.25, 7.17) \text{ km s}^{-1}$  (Dehnen & Binney 1998). These components are positive if  $u_{\odot}$  points radially away from the Galactic center,  $v_{\odot}$  points in the direction of Galactic rotation and  $w_{\odot}$  is directed towards the Galactic north pole.

Although the matter was not addressed here, the values presented in table 10 can be used to determine the orbit of the LMC and therefore study possible past and future interactions of the LMC with other Local Group galaxies.

If we assume that the LMC is gravitationally bound to, and in an elliptical orbit, around the Galaxy, and that the mass of the Galaxy is contained within 50 kpc of the galactic center, we can make an estimate of the lower limit of its mass through the expression:

$$M_G = (r_{\text{LMC}}/2G)[V_{\text{gc}, r}^2 + V_{\text{gc}, t}^2 (1 - r_{\text{LMC}}^2/r_a^2)]/(1 - r_{\text{LMC}}/r_a)$$

where  $r_a$  is the LMC's apogalacticon distance and  $r_{\text{LMC}}$  its present distance.

For  $r_a = 300 \text{ kpc}$  (Lin et al. 1995) we obtain  $M_G$  values of :  $(8.2 \pm 1.3)$ ,  $(9.9 \pm 1.6)$ ,  $(3.0 \pm 0.8)$  and  $(12 \pm 2) \times 10^{11} \mathcal{M}_{\odot}$ , for the fields, Q0459-6427, Q0557-6713, Q0558-6707 and Q0615-6615, respectively. The above values result in a weighted average of:  $\langle M_G \rangle = (5.9 \pm 0.6) \times 10^{11} \mathcal{M}_{\odot}$  for the estimated mass of our Galaxy enclosed within 50 kpc.

To evaluate the effect of the rotational velocity of the LMC on the determination of the mass of our galaxy, we also carried out calculations using the extreme values  $v_{\Phi} = 0 \text{ km s}^{-1}$  (zero rotation) and  $v_{\Phi} = 90 \text{ km s}^{-1}$ . The weighted mass averages for 0 and  $90 \text{ km s}^{-1}$  resulted to be  $(5.6 \pm 0.6) \times 10^{11}$  and  $(6.3 \pm 0.6) \times 10^{11} \mathcal{M}_{\odot}$ , respectively. Our results are summarized in Table 11.

It should be noted that (although slightly larger), all our values for  $M_G$  are compatible with the recent theoretical  $5.5 \times 10^{11} \mathcal{M}_{\odot}$  upper mass limit of the Galaxy given by Sakamoto et al. (2003). They are also compatible with the assumption that the LMC is bound to the Galaxy.

## 6. DISCUSSION

### 6.1. The ALP-PAM Discrepancy

Given the implications of the result obtained by ALP for the PM of the LMC, in relation to our understanding of the interactions between the Galaxy and the Magellanic Clouds (see,

e.g, Momany & Zaggia, 2005), and the reality of streams of galaxies with similar orbits around the Galaxy (see, e.g, Piatek et al., 2005), the main objective of the present work was to clarify the discrepancy between the previous determinations of the PM of the LMC by our group: the ”ALP-PAM Discrepancy”. In this section, we further elaborate on some of the thoughts originally proposed in PAM, in order to explain the discrepancy of ALP, originally with PAM, and now also with the new result presented in this paper.

First, the fact that the observations used here were made with essentially the same equipment and instrumental set-up as those by ALP, precludes any arguments relating the observed discrepancy to the existence of systematic errors in the observational data. Such errors would affect our data in the same way as those of ALP.

Second (as explained in §2), in the reduction process of the ALP and PAM data incorporated in the present work we adopted the same QSO and reference stars centroid coordinates (x,y) used in those works. Furthermore, the new data included in the present calculations was processed using the same procedure used in ALP to obtain the (x,y) coordinates. Therefore, the centroid coordinates should not be a source of a systematic error either.

The subsequent procedures to obtain the PM were also basically the same, the sole exception being the inclusion of a quadratic term in the transformation equations used for the registration (also included in PAM’s equations, but not in ALP’s). Tests carried out using ALP’s data alone showed however that the effect of including quadratic terms is marginal (as was suspected), and does not account for the observed discrepancy.

Considering that our current result -which includes re-processed data from ALP- agrees quite well with measurements by other groups, we conclude that ALP’s results might be affected by an unidentified systematic error in Decl. Since in the present work we used ALP’s unmodified (x,y) coordinates, we believe that this error could have originated in the processing of the Decl. PM instead of the coordinates themselves.

It should be pointed out that the UCAC2-based result from Momany & Zaggia (2005), which is consistent with that from ALP, is currently also considered to be affected by an as yet unidentified systematic error (Momany & Zaggia, 2005; Kallivayalil et al., 2005).

We would finally like to note that our new result for field Q0459-6427 is consistent with PAM.

## 6.2. Membership of the LMC to a Stream

Lynden-Bell & Lynden-Bell (1995), have proposed that the LMC, together with the SMC, Draco and Ursa Minor, and possibly Carina and Sculptor, define a stream of galaxies with similar orbits around our galaxy. Their models predict a PM for each of member of the stream, which can be compared to their measured PM to evaluate the reality of the stream.

For the LMC they predict PM components of  $[\mu_\alpha \cos \delta, \mu_\delta] = [+1.5, 0]$  mas yr<sup>-1</sup>, giving a total PM of  $\mu = +1.5$  mas yr<sup>-1</sup>, with a position angle of  $\theta = 90^\circ$ . A comparison of this prediction with our result  $[\mu = (+2.0 \pm 0.1)$  mas yr<sup>-1</sup>,  $\theta = (62.4 \pm 3.1)^\circ]$ , shows that our measured values of  $\mu$  and  $\theta$  are, respectively,  $5.1\sigma$  and  $8.9\sigma$  away from the predicted values. This result indicates that the LMC does not seem to be a member of the above stream (it is worth mentioning that Piatek et al. (2005), using HST data, have concluded that Ursa Minor is not a member of this stream).



MHP is grateful of the support by the Universidad de Tarapacá research fund (project # 4722-02). EC and RAM acknowledge support by the Fondo Nacional de Investigación Científica y Tecnológica (proyecto No. 1050718, Fondecyt) and by the Chilean Centro de Astrofísica FONDAP (No. 15010003). It is also a pleasure to thank T. Martínez for helping with data processing.

We would like to thank the referee, Dr. S. Piatek, for his constructive comments.

## REFERENCES

- Anguita, C., Loyola, P., & Pedreros, M. H. 2000, *AJ*, 120, 845
- Dehnen, W., & Binney, J. J. 1998, *MNRAS*, 298, 387
- Drake, A. J., Cook, K. H., Alcock, C., Axelrod, T. S., Geha, M., & MACHO Collaboration 2001, *Bulletin of the American Astronomical Society*, 33, 1379
- Gardiner, L. T., Sawa, T., & Fujimoto, M. 1994, *MNRAS*, 266, 567
- Jones, B. F., Klemola, A. R., & Lin, D. N. C. 1994, *AJ*, 107, 1333
- Kallivayalil, N., van der Marel, R. P., Alcock, C., Axelrod, T., Cook, K. H., Drake, A. J., & Geha, M. 2005, *ArXiv Astrophysics e-prints*, arXiv:astro-ph/0508457
- Kroupa, P., & Bastian, U. 1997, *New Astronomy*, 2, 77
- Kroupa, P., Röser, S., & Bastian, U. 1994, *MNRAS*, 266, 412
- Lin, D. N. C., Klemola, A. R., & Jones, B. F. 1995, *ApJ*, 439, 652
- Lynden-Bell, D., & Lynden-Bell, R. M. 1995, *MNRAS*, 275, 429
- Momany, Y., & Zaggia, S. 2005, *A&A*, 437, 339
- Pedreros, M. H., Anguita, C., & Maza, J. 2002, *AJ*, 123, 1971
- Piatek, S., Pryor, C., Bristow, P., Olszewski, E. W., Harris, H. C., Mateo, M., Minniti, D., & Tinney, C. G. 2005, *AJ*, 130, 95
- Röser, S., & Bastian, U. 1993, *Heidelberg: Spektrum, Akademischer Verlag*, —c1993
- Sakamoto, T., Chiba, M., & Beers, T. C. 2003, *A&A*, 397, 889
- Stetson, P. B. 1987, *PASP*, 99, 191
- Schweitzer, A. E., Cudworth, K. M., Majewski, S. R., & Suntzeff, N. B. 1995, *AJ*, 110, 2747
- Zacharias, N., Urban, S. E., Zacharias, M. I., Wycoff, G. L., Hall, D. M., Monet, D. G., & Rafferty, T. J. 2004, *AJ*, 127, 3043



### Figure Captions

**Figure 1.** Residual proper motion maps for the reference stars listed in Tables 3-6. The dispersion around the mean is  $\pm 0.34$ ,  $\pm 0.79$ ,  $\pm 0.54$ , and  $\pm 0.41$  mas yr $^{-1}$  in R.A., and  $\pm 0.52$ ,  $\pm 0.71$ ,  $\pm 0.58$ ,  $\pm 0.62$  mas yr $^{-1}$  in Decl., for Q0459-6427, Q0557-6713, Q0558-6707 and Q0615-6615, respectively.

**Figure 2a.** Relative positions in Right Ascension ( $\Delta\alpha\cos\delta$ ) *vs.* epoch of observation for the studied fields. The values of  $\Delta\alpha\cos\delta$  represent the individual positions of the QSO on different CCD frames relative to the barycenter of the SRF. Symbol sizes are proportional to the number of times the measurements yielded the same coordinate value for a particular epoch (extra small, small, medium, large, and extra large sizes indicate 1 through 5 measurements per epoch, respectively). The best-fit straight lines from linear regression analyses on the data are also shown.

**Figure 2b.** Relative positions in declination ( $\Delta\delta$ ) *vs.* epoch of observation for the studied fields. The values of  $\Delta\delta$  represent the individual positions of the QSO on different CCD frames relative to the barycenter of the SRF. Symbol sizes and best-fit straight lines as described in Fig 2a.

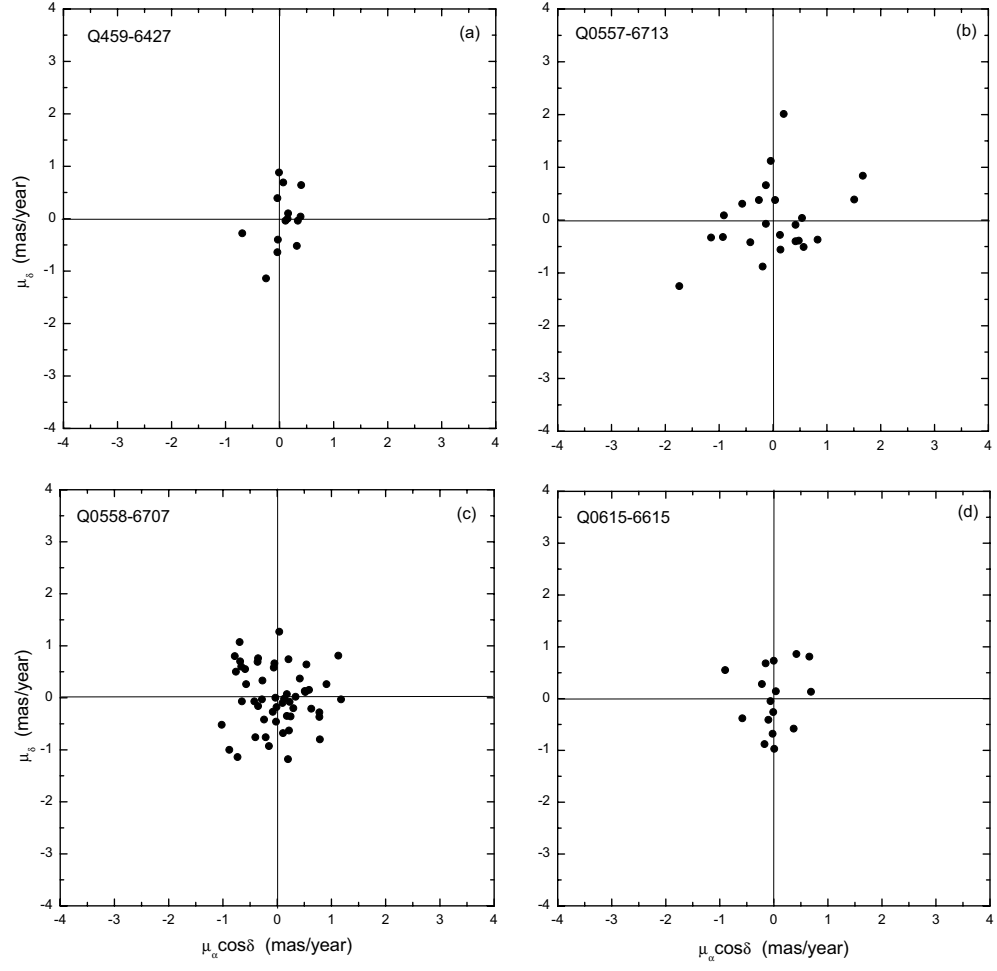
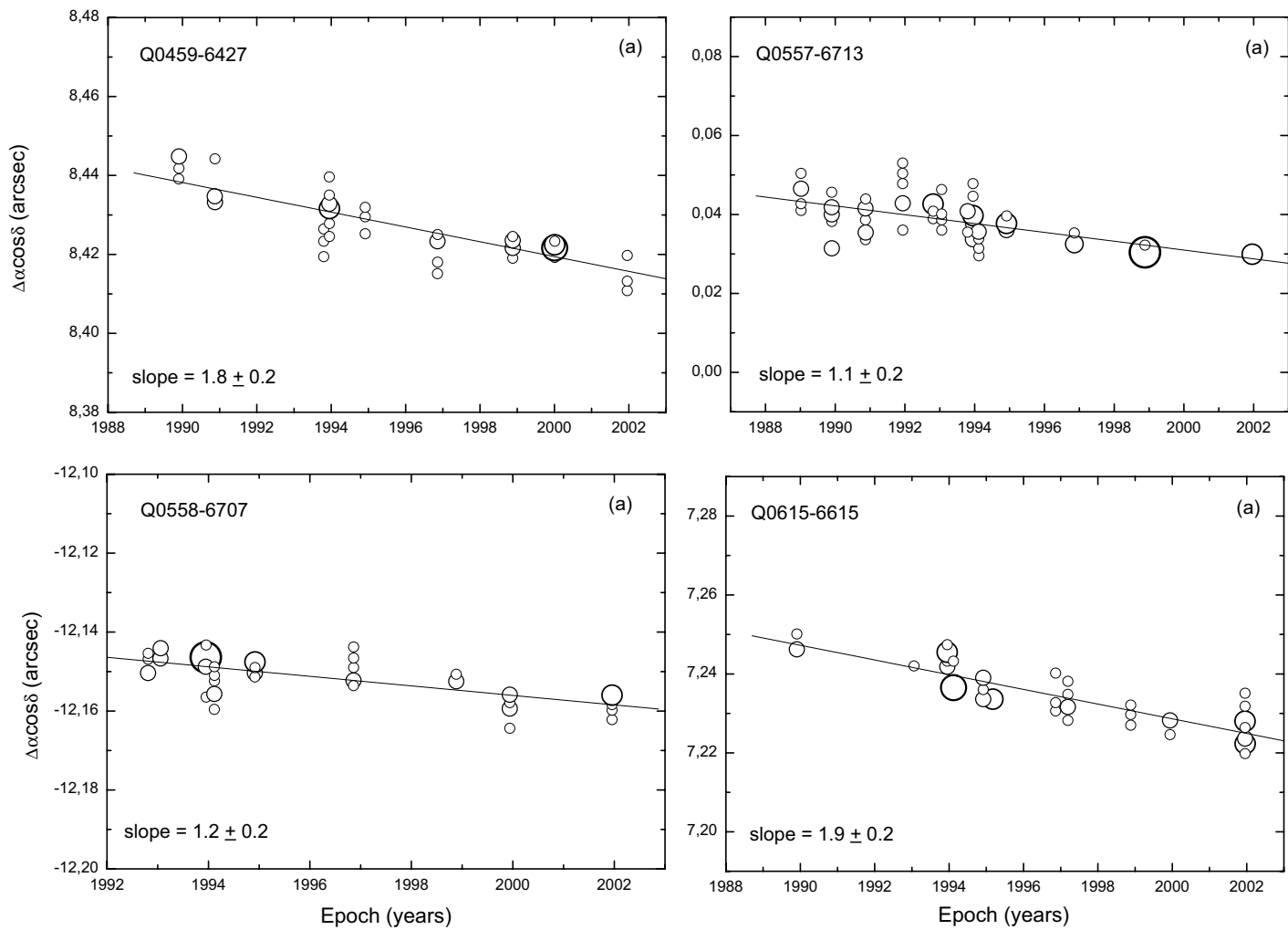


Fig. 1.—



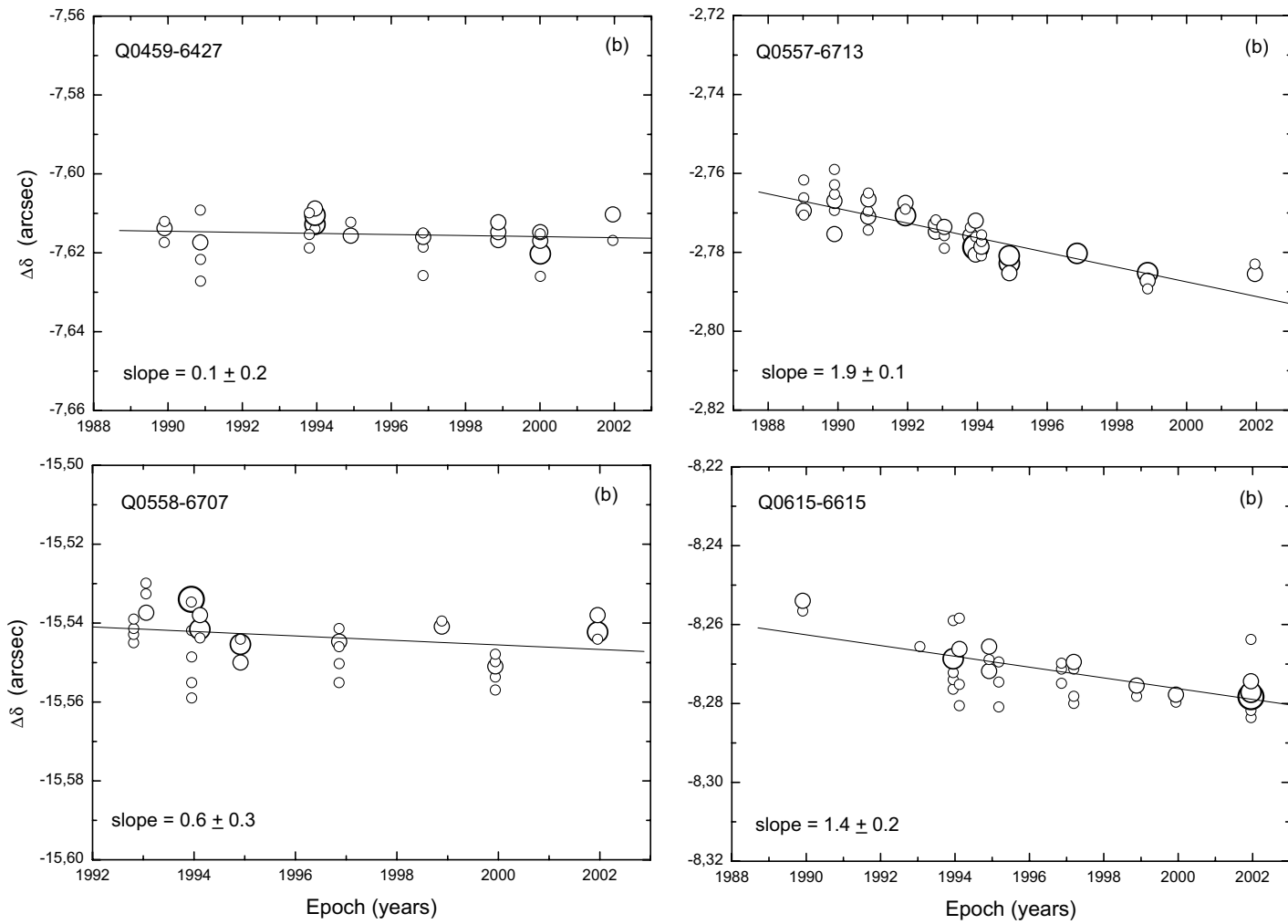


Table 1  
Previous determinations of the LMC proper motion using the quasar method

Source	$\mu_\alpha \cos \delta$ mas yr <sup>-1</sup>	$\mu_\delta$ mas yr <sup>-1</sup>	Weighted Mean from
ALP(LMC center)	+1.7 ± 0.2	+2.9 ± 0.2	3 fields
PAM (LMC center)	+2.0 ± 0.2	+0.4 ± 0.2	1 field

Table 2  
Observational material for the LMC QSO fields

Field	Old Data				New Data		
	Source	Epochs	# Frames	Epoch Range	Epochs	# Frames	Epoch Range
Q0459-6427	PAM	8	44	1989.91–2000.01	1	3	2001.96
Q0557-6713	ALP	11	61	1989.02–1996.86	2	11	1998.88–2001.96
Q0558-6707	ALP	6	32	1992.81–1996.86	3	19	1998.88–2001.96
Q0615-6615	ALP	8	32	1989.90–1997.19	3	18	1998.88–2001.96

Table 3  
Local Reference System for the Q0459–6427 field

Star <sup>(a)</sup> ID	$\mu_\alpha \cos \delta$ mas yr <sup>-1</sup>	$\sigma$ mas yr <sup>-1</sup>	$\mu_\delta$ mas yr <sup>-1</sup>	$\sigma$ mas yr <sup>-1</sup>	V mag	B–V mag	V–R mag
1	0.0	0.3	+0.9	0.2	18.71	0.95	0.52
2	–0.7	0.3	–0.3	0.4	19.01	0.67	0.38
3	+0.6	0.2	–0.4	0.2	19.02	0.86	0.47
4	0.0	0.3	0.0	0.3	18.88	0.96	0.52
5	0.0	0.3	+0.6	0.3	18.71	0.98	0.54
6	–0.1	0.2	–0.4	0.2	18.22	1.03	0.58
7	+0.1	0.2	+0.1	0.2	18.08	1.03	0.57
8	0.0	0.5	–0.1	0.4	17.98	0.89	0.52
9	+0.1	0.3	–0.6	0.4	19.18	0.84	0.43
10	+0.3	0.1	0.0	0.2	17.94	1.15	0.63
11	0.0	0.3	+0.4	0.3	18.64	0.91	0.50
12	–0.3	0.3	–1.2	0.3	19.03	0.88	0.48
13	+0.4	0.3	+0.6	0.3	18.98	0.86	0.48
14	–0.7	0.3	+0.1	0.3	18.66	0.23	0.03
15	+0.2	0.1	–0.1	0.2	17.70	1.08	0.59
16	+0.4	0.2	+0.3	0.2	16.70	1.43	0.82
17	–0.3	0.2	+0.3	0.2	19.17	0.95	0.51

<sup>(a)</sup>Star IDs are the same as those in PAM



Table 4  
Local Reference System for the Q0557–6713 field

Star <sup>(a)</sup>	$\mu_\alpha \cos \delta$	$\sigma$	$\mu_\delta$	$\sigma$	V	B–V	V–R
ID	mas yr <sup>−1</sup>	mas yr <sup>−1</sup>	mas yr <sup>−1</sup>	mas yr <sup>−1</sup>	mag	mag	mag
1	−0.1	0.1	−0.1	0.2	17.07	−0.07	−0.04
2	+0.5	0.2	0.0	0.1	17.75	1.14	0.56
3	−0.1	0.2	+0.7	0.2	18.35	0.84	0.45
4	+0.2	0.3	+2.0	0.3	18.64	0.68	0.38
5	−0.2	0.4	−0.9	0.2	16.93	1.13	0.55
6	+0.6	0.2	−0.5	0.2	17.72	1.22	0.62
7	−0.9	0.3	−0.3	0.3	18.73	1.09	0.48
8	−1.2	0.2	−0.3	0.2	17.29	0.83	0.46
9	+1.5	0.3	+0.4	0.6	18.52	1.00	0.52
10	−1.7	0.6	−1.2	0.3	18.28	0.00	−0.05
11	+0.4	0.2	−0.4	0.2	17.34	1.17	0.56
12	−0.6	0.3	+0.3	0.2	18.66	1.00	0.48
13	−0.4	0.2	−0.4	0.2	18.23	0.75	0.37
14	+1.7	0.3	+0.8	0.3	18.13	0.82	0.42
15	+0.8	0.3	−0.4	0.2	18.48	0.80	0.43
16	+0.4	0.2	−0.1	0.2	18.26	1.09	0.53
17	+0.1	0.2	−0.6	0.2	17.78	0.95	0.51
18	+0.5	0.4	−0.4	0.3	17.57	−0.12	−0.06
19	+0.1	0.1	−0.3	0.2	17.21	1.19	0.63
20	−0.9	0.3	+0.1	0.3	18.69	0.99	0.50
21	−0.3	0.1	+0.4	0.2	17.30	0.77	0.38
22	0.0	0.3	+1.2	0.3	18.05	−0.08	−0.08
23	0.0	0.1	+0.4	0.2	16.23	−0.17	−0.09

<sup>(a)</sup>Star IDs are the same as those in ALP

Table 5  
Local Reference System for the Q0558–6707 field

Star <sup>(a)</sup> ID	$\mu_\alpha \cos \delta$ mas yr <sup>-1</sup>	$\sigma$ mas yr <sup>-1</sup>	$\mu_\delta$ mas yr <sup>-1</sup>	$\sigma$ mas yr <sup>-1</sup>	V mag	B–V mag	V–R mag
1	+0.8	0.5	–0.8	0.7	18.94	0.84	0.44
2	–0.7	0.4	–1.1	0.4	16.44	1.78	0.91
3	+0.2	0.3	–1.2	0.4	17.88	0.90	0.46
4	+0.8	0.5	–0.4	0.6	18.94	0.85	0.46
5	–0.9	0.3	–1.0	0.7	19.01	0.90	0.44
6	–0.7	0.2	+0.6	0.2	18.30	0.88	0.49
7	+0.5	0.2	+0.1	0.3	17.78	1.18	0.62
8	+1.1	0.4	+0.8	0.4	18.36	....	–0.11
9	+0.2	0.2	–0.4	0.2	17.39	1.34	0.70
10	+0.5	0.2	+0.1	0.3	18.43	0.86	0.46
11	–0.8	0.2	+0.8	0.2	17.79	1.13	0.59
12	0.0	0.2	0.0	0.3	18.59	0.88	0.45
13	–0.2	0.3	–0.4	0.4	18.34	–0.02	0.00
14	0.0	0.4	+0.7	0.4	18.20	0.01	–0.01
15	–0.6	0.2	+0.6	0.2	17.44	1.26	0.66
16	–0.7	0.4	+0.7	0.5	19.00	0.91	0.49
17	–0.7	0.3	+1.1	0.3	18.48	0.69	0.40
18	–0.1	0.5	+0.6	0.6	18.98	0.90	0.48
19	+0.2	0.3	+0.7	0.4	18.32	–0.13	–0.02
20	–0.4	0.4	+0.8	0.5	19.00	0.87	0.49
21	+0.4	0.3	+0.4	0.5	18.84	0.91	0.48
22	–0.3	0.4	+0.3	0.4	18.83	0.91	0.48
23	–0.4	0.4	–0.2	0.2	16.29	0.02	0.17
24	0.0	0.2	–0.2	0.2	17.56	1.27	0.67
25	+0.2	0.2	–0.1	0.3	17.69	1.15	0.60

<sup>(a)</sup>Star IDs are the same as those in ALP

Table 5  
Local Reference System for the Q0558–6707 field(continued)

Star <sup>(a)</sup> ID	$\mu_\alpha \cos \delta$ mas yr <sup>-1</sup>	$\sigma$ mas yr <sup>-1</sup>	$\mu_\delta$ mas yr <sup>-1</sup>	$\sigma$ mas yr <sup>-1</sup>	V mag	B–V mag	V–R mag
26	+0.2	0.2	+0.1	0.4	18.72	1.20	0.57
27	–0.1	0.2	–0.3	0.3	18.66	1.00	0.54
28	–0.6	0.2	+0.3	0.2	17.31	1.25	0.64
29	+0.6	0.4	–0.2	0.4	18.92	0.89	0.47
30	–0.4	0.3	–0.1	0.3	18.18	1.25	0.59
31	+0.8	0.3	–0.3	0.3	18.55	1.01	0.54
32	+0.2	0.3	–0.4	0.3	18.07	1.12	0.61
33	+0.6	0.2	+0.2	0.2	17.12	1.46	0.76
34	+0.9	0.8	+0.3	0.8	18.68	0.84	0.48
35	+0.2	0.2	–0.6	0.2	17.42	0.90	0.47
36	+0.1	0.3	–0.7	0.4	18.75	0.83	0.45
37	–0.4	0.3	–0.8	0.2	18.65	1.27	0.56
38	0.0	0.2	–0.5	0.2	17.89	1.18	0.60
39	+0.1	0.4	–0.1	0.4	19.12	0.92	0.50
40	–0.7	0.4	–0.1	0.4	19.05	0.88	0.50
41	+0.3	0.2	–0.2	0.4	18.35	0.01	0.02
42	–0.2	0.2	–0.9	0.5	18.58	0.89	0.50
43	+0.1	0.2	0.0	0.2	17.45	1.32	0.68
44	+0.3	0.5	0.0	0.6	19.01	0.85	0.49
45	0.0	0.3	+1.3	0.3	18.46	0.66	0.43
46	–0.8	0.3	+0.5	0.4	19.05	0.86	0.52
47	–0.4	0.4	+0.7	0.6	19.04	1.01	0.54
48	+0.5	0.2	+0.6	0.3	16.81	0.08	0.06
49	+1.2	0.4	0.0	0.3	19.04	0.83	0.49
50	–1.0	0.3	–0.5	0.3	17.76	1.07	0.57
51	–0.2	0.3	–0.8	0.3	18.16	0.83	0.48
52	–0.3	0.4	0.0	0.5	18.93	0.89	0.46

<sup>(a)</sup>Star IDs are the same as those in ALP

Table 6  
Local Reference System for the Q0615–6615 field

Star <sup>(a)</sup> ID	$\mu_\alpha \cos \delta$ mas yr <sup>-1</sup>	$\sigma$ mas yr <sup>-1</sup>	$\mu_\delta$ mas yr <sup>-1</sup>	$\sigma$ mas yr <sup>-1</sup>	V mag	B–V mag	V–R mag
1	0.0	0.2	+0.1	0.4	18.95	0.87	0.53
2	0.0	0.2	+0.7	0.3	18.29	0.83	0.47
3	–0.1	0.2	–0.4	0.3	17.46	0.75	0.43
4	0.0	0.3	–1.0	0.4	19.14	0.61	0.41
5	–0.2	0.2	+0.3	0.2	18.23	0.76	0.45
6	+0.4	0.3	+0.9	0.3	19.00	0.98	0.56
7	–0.6	0.2	–0.4	0.2	19.07	0.65	0.42
8	+0.7	0.2	+0.1	0.2	18.37	0.89	0.53
9	–0.2	0.4	+0.7	0.5	18.98	0.84	0.49
10	–0.2	0.3	–0.9	0.4	18.85	0.85	0.48
11	0.0	0.3	–0.3	0.4	18.97	....	0.73
12	0.0	0.2	–0.7	0.2	18.25	1.07	0.53
13	–0.1	0.2	0.0	0.3	17.59	1.04	0.65
14	+0.7	0.2	+0.8	0.2	18.33	1.00	0.57
15	+0.4	0.4	–0.6	0.5	19.36	0.90	0.50
16	–0.9	0.4	+0.6	0.5	19.29	0.81	0.47

<sup>(a)</sup>Star IDs are the same as those in ALP

Table 7  
Mean barycentric positions of quasars in the LMC

Epoch	$\Delta\alpha \cos\delta$	$\sigma$	$\Delta\delta$	$\sigma$	N	CCD chip
	arcsec	mas	arcsec	mas		
Q0459-6427:						
1989.907	8.443	1.4	−7.614	1.1	4	RCA No.5
1990.872	8.434	0.3	−7.615	2.7	3	Tek No. 4
1990.878	8.438	5.8	−7.624	2.8	2	RCA No.5
1993.800	8.423	2.0	−7.615	2.6	3	Tek1024 No.1
1993.953	8.432	1.4	−7.611	0.7	9	Tek1024 No.2
1994.916	8.429	2.0	−7.615	1.1	3	Tek1024 No.2
1996.860	8.421	1.9	−7.618	2.0	5	Tek 2048 No.4
1998.881	8.422	0.8	−7.615	0.8	6	Tek1024 No.2
2000.010	8.422	0.4	−7.618	1.2	9	Tek1024 No.2
2001.961	8.416	2.1	−7.612	2.9	3	Tek1024 No.2
Q0557-6713:						
1989.024	0.045	1.6	−2.768	1.6	5	RCA No.5
1989.905	0.039	1.8	−2.768	1.9	8	RCA No.5
1990.872	0.037	1.6	−2.772	1.0	4	Tek No. 4
1990.878	0.040	2.7	−2.766	0.5	3	RCA No.5
1991.938	0.046	2.5	−2.769	0.7	6	Tek1024 No.1
1992.812	0.042	0.7	−2.774	0.6	5	Tek2048 No.1
1993.055	0.040	2.2	−2.776	1.3	4	Tek1024 No.1
1993.800	0.039	1.8	−2.775	0.7	3	Tek1024 No.1
1993.953	0.039	1.5	−2.777	1.1	9	Tek1024 No.2
1994.119	0.033	1.2	−2.778	0.9	5	Tek1024 No.2
1994.918	0.036	0.8	−2.783	0.7	8	Tek1024 No.2
1996.862	0.033	0.9	−2.780	0.3	3	Tek 2048 No.4
1998.883	0.031	0.3	−2.786	0.7	6	Tek1024 No.2
2001.961	0.030	0.3	−2.785	0.9	3	Tek1024 No.2

Table 7 (continued)  
Mean barycentric positions of quasars in the LMC

Epoch	$\Delta\alpha \cos\delta$ arcsec	$\sigma$ mas	$\Delta\delta$ arcsec	$\sigma$ mas	N	CCD chip
Q0558-6707:						
1992.813	−12.148	1.3	−15.542	1.3	4	Tek2048 No.1
1993.058	−12.145	0.8	−15.534	1.8	4	Tek1024 No.1
1993.953	−12.148	1.2	−15.542	3.4	9	Tek1024 No.2
1994.118	−12.154	1.6	−15.541	1.0	6	Tek1024 No.2
1994.918	−12.149	0.6	−15.547	0.9	7	Tek1024 No.2
1996.863	−12.150	1.6	−15.547	2.0	6	Tek 2048 No.4
1998.886	−12.152	0.7	−15.540	0.5	3	Tek1024 No.2
1999.942	−12.159	1.3	−15.552	1.3	6	Tek1024 No.2
2001.958	−12.158	1.1	−15.541	1.1	6	Tek1024 No.2
Q0615-6615:						
1989.908	7.248	1.3	−8.255	0.9	3	RCA No.5
1993.058	7.242		−8.266		1	Tek1024 No.1
1993.953	7.244	0.8	−8.270	2.1	7	Tek1024 No.2
1994.120	7.238	1.3	−8.269	3.9	5	Tek1024 No.2
1994.920	7.236	1.2	−8.269	1.4	5	Tek1024 No.2
1995.178	7.234	0.2	−8.275	3.3	3	Tek1024 No.2
1996.864	7.234	2.9	−8.272	1.5	3	Tek 2048 No.4
1997.194	7.233	1.7	−8.274	2.2	5	Tek1024 No.2
1998.886	7.230	1.5	−8.276	1.0	3	Tek1024 No.2
1999.942	7.227	1.2	−8.278	0.8	3	Tek1024 No.2
2001.960	7.226	1.3	−8.277	1.4	12	Tek1024 No.2

Table 8  
Proper Motion of the LMC (as measured)

Field ID	$\mu_\alpha \cos(\delta)$ mas yr <sup>−1</sup>	$\mu_\delta$ mas yr <sup>−1</sup>	# Frames	Epochs	Epoch Range
Q0459-6427	1.8 ± 0.2	0.1 ± 0.2	47	9	1989.91–2001.96
Q0557-6713	1.1 ± 0.2	1.9 ± 0.1	72	13	1989.02–2001.96
Q0558-6707	1.2 ± 0.2	0.6 ± 0.3	51	9	1992.81–2001.96
Q0615-6615	1.9 ± 0.2	1.4 ± 0.2	50	11	1989.90–2001.96

Table 9  
High precision determinations of the proper motion of the LMC

Source	$\mu_\alpha \cos(\delta)$ mas yr <sup>-1</sup>	$\mu_\delta$ mas yr <sup>-1</sup>	Proper Motion System
Kroupa, Röser & Bastian 1994 (Field)	+1.3 ± 0.6	+1.1 ± 0.7	PPM
Jones et al. 1994	+1.37 ± 0.28	−0.18 ± 0.27	Galaxies
Kroupa & Bastian 1997 (Field)	+1.94 ± 0.29	−0.14 ± 0.36	Hipparcos
ALP	+1.7 ± 0.2	+2.9 ± 0.2	Quasars
PAM	+2.0 ± 0.2	+0.4 ± 0.2	Quasars
Drake et al. 2001	+1.4 ± 0.4	+0.38 ± 0.25	Quasars
Kallivayalil et al. 2005	+2.03 ± 0.08	+0.44 ± 0.05	Quasars
This work (Field) <sup>a</sup>	+1.5 ± 0.1	+1.4 ± 0.1	Quasars
This work <sup>a</sup>	+1.8 ± 0.1	+0.9 ± 0.1	Quasars

<sup>(a)</sup> Weighted mean of our four QSO fields

Table 10  
Proper Motion and Space Velocity Results for the LMC

Parameter	Q0459-6427	Q0557-6713	Q0558-6707	Q0615-6615
$\Delta\mu_\alpha \cos \delta$ , rotation correction (mas yr <sup>-1</sup> )	+0.17	+0.11	+0.11	+0.12
$\Delta\mu_\delta$ , rotation correction (mas yr <sup>-1</sup> )	+0.09	−0.18	−0.18	−0.18
$\mu_\alpha^{LMC} \cos \delta$ , LMC centered (mas yr <sup>-1</sup> )	1.9 ± 0.2	1.5 ± 0.2	1.4 ± 0.2	2.2 ± 0.2
$\mu_\delta^{LMC}$ , LMC centered (mas yr <sup>-1</sup> )	0.5 ± 0.2	1.5 ± 0.1	0.2 ± 0.2	0.7 ± 0.2
$\mu_\alpha^{GRF} \cos \delta$ (mas yr <sup>-1</sup> )	1.4 ± 0.1	1.0 ± 0.1	0.9 ± 0.1	1.7 ± 0.1
$\mu_\delta^{GRF}$ (mas yr <sup>-1</sup> )	0.4 ± 0.2	1.3 ± 0.1	0.1 ± 0.3	0.6 ± 0.2
$\mu_l^{GRF} \cos b$ (mas yr <sup>-1</sup> )	−0.6 ± 0.2	−1.5 ± 0.1	−0.3 ± 0.3	−0.9 ± 0.2
$\mu_b^{GRF}$ (mas yr <sup>-1</sup> )	1.4 ± 0.1	0.7 ± 0.1	0.8 ± 0.1	1.5 ± 0.1
$\Pi$ , velocity component (km s <sup>-1</sup> )	252 ± 25	215 ± 23	171 ± 28	292 ± 23
$\Theta$ , velocity component (km s <sup>-1</sup> )	93 ± 41	319 ± 31	27 ± 63	160 ± 45
$Z$ , velocity component (km s <sup>-1</sup> )	234 ± 25	109 ± 24	135 ± 26	274 ± 22
$V_{gc,r}$ , radial velocity (km s <sup>-1</sup> )	80 ± 23	118 ± 22	68 ± 24	92 ± 20
$V_{gc,t}$ , transverse velocity (km s <sup>-1</sup> )	347 ± 27	382 ± 30	209 ± 27	421 ± 27

Table 11  
Mass of the Galaxy for three LMC rotational velocities

Parameter	Q0459-6427	Q0557-6713	Q0558-6707	Q0615-6615
$v_\Phi = 50 \text{ km s}^{-1}$				
$V_{\text{gc},r}$ , radial velocity ( $\text{km s}^{-1}$ )	$80 \pm 23$	$118 \pm 22$	$68 \pm 24$	$92 \pm 20$
$V_{\text{gc},t}$ , transverse velocity ( $\text{km s}^{-1}$ )	$347 \pm 27$	$382 \pm 30$	$209 \pm 27$	$421 \pm 27$
$M_G$ , mass of the Galaxy in $10^{11} \times \mathcal{M}_\odot$	$(8.2 \pm 1.3)$	$(9.9 \pm 1.6)$	$(3.0 \pm 0.8)$	$(12 \pm 2)$
$v_\Phi = 0 \text{ km s}^{-1}$				
$V_{\text{gc},r}$ , radial velocity ( $\text{km s}^{-1}$ )	$75 \pm 23$	$126 \pm 22$	$75 \pm 24$	$99 \pm 20$
$V_{\text{gc},t}$ , transverse velocity ( $\text{km s}^{-1}$ )	$305 \pm 26$	$408 \pm 30$	$198 \pm 33$	$420 \pm 30$
$M_G$ , mass of the Galaxy in $10^{11} \times \mathcal{M}_\odot$	$(6.3 \pm 1.1)$	$(11 \pm 2)$	$(2.7 \pm 0.9)$	$(12 \pm 2)$
$v_\Phi = 90 \text{ km s}^{-1}$				
$V_{\text{gc},r}$ , radial velocity ( $\text{km s}^{-1}$ )	$83 \pm 23$	$112 \pm 22$	$62 \pm 24$	$86 \pm 20$
$V_{\text{gc},t}$ , transverse velocity ( $\text{km s}^{-1}$ )	$381 \pm 27$	$364 \pm 29$	$225 \pm 26$	$425 \pm 25$
$M_G$ , mass of the Galaxy in $10^{11} \times \mathcal{M}_\odot$	$(9.9 \pm 1.4)$	$(9.0 \pm 1.5)$	$(3.4 \pm 0.8)$	$(12 \pm 2)$